Distributed Low Voltage Ride-Through Operation of Power Converters in Grid-Connected Microgrids under Voltage Sags

Zhao, Xin; Meng, Lexuan; Dragicevic, Tomislav; Savaghebi, Mehdi; Guerrero, Josep M.; Quintero, Juan Carlos Vasquez; Wu, Xiaohua

Published in:
Proceedings of the 41th Annual Conference of IEEE Industrial Electronics Society, IECON 2015

DOI (link to publication from Publisher):
10.1109/IECON.2015.7392379

Publication date:
2015

Distributed Low Voltage Ride-Through Operation of Power Converters in Grid-Connected Microgrids under Voltage Sags

Xin Zhao, Lexuan Meng, Tomislav Dragicevic, Mehdi Savaghebi, Josep M. Guerrero, Juan C. Vasquez
Department of Energy Technology
Aalborg University, Denmark
{xzh, lme, tdr, mes, joz, juq}@et.aau.dk

Xiaohua Wu
School of Automation
Northwestern Polytechnical University
Xi'an, China
wxh@nwpu.edu.cn

***Abstract*—With the increasing penetration of renewable energy, microgrids (MGs) have gained a great attention over the past decade. However, a sudden cut out of the MGs due to grid fault may lead to adverse effects to the grid. As a consequence, reactive power injection provided by MGs is preferred since it can make the MG a contributor in smooth ride through the faults. In this paper, a reactive power support strategy using droop controlled converters is proposed to aid MG riding through three phase symmetrical voltage sags. In such a case, the MGs should inject reactive power to the grid to boost the voltage in all phases at AC common bus. However, since the line admittances from each converter to point of common coupling (PCC) are not identical, the injected reactive power may not be equally shared. In order to achieve low voltage ride through (LVRT) capability along with a good power sharing accuracy, a hierarchical control strategy is proposed in this paper. Droop control and virtual impedance is applied in primary control loop while secondary control loop is based on dynamic consensus algorithm (DCA). Experiments are conducted to verify the effectiveness of the proposed control strategy.**

Keywords—microgrids; droop control; low voltage ride through; dynamic consensus algorithm

I. INTRODUCTION

Driven by the economic and environmental issues, combined heat and power (CHP), and distributed energy resources (DERs), such as wind turbines (WT) and photovoltaic (PV) arrays are combined with advanced power electronics technology systems and integrated into future networks such as Microgrids (MG) [1]. MGs not only can provide electricity to the local loads, but also deliver electricity with higher reliability and quality to the grid.

Recently, due to the continuously increasing capacity of MGs, some countries had revised their grid codes to require distributed generation (DG) to provide ancillary services to the grid, e.g. reactive power injection, load following, backup service and elimination of power quality (*PQ*) disturbances [2-4]. Unfortunately, the published grid requirements mainly focus on wind farms connected to medium or high voltage grid, in a near future, these requirements could be extended to low voltage MGs [5].

Germany and Denmark have already published the LVRT and reactive current injection requirements for grid connected DGs in 2007 and 2010 respectively. The German E.ON NetZ high voltage LVRT requirements [3] are shown in Fig. 1 and 2. These requirements can also be applied to low voltage grid, since LVRT in low voltage grid has the similar concepts.

It can be seen in Fig. 1 that only when the grid voltage falls below the curve, the DGs are allowed to disconnect with the grid. Otherwise, DGs should inject a certain amount of reactive power as defined in Fig. 2. It is clear that when the grid voltage is lower than $0.9V_N$, 1% drop of the grid voltage requires at least k% increase of the rated current.

Conventionally, LVRT in PV plants and wind farms are achieved by means of controlling the grid-interactive converter as a current source in which the phase is sensed from the grid voltage by using phase-locked-loop, meanwhile a current loop ensures the accurate amount of power injection and the current quality issues [6-8]. However, the exact methodologies on how to achieve LVRT in a grid connected MGs, where droop controlled converters are widely adopted, are rarely studied. In [9], a LVRT strategy for droop control based single phase converters is proposed to inject reactive power during voltage sags. But, if the transmission lines are un-identical because of different distances, the reactive power injected cannot be well shared, and then cause unequal current sharing. In this case, the converter locate closer to the PCC have to supply more reactive current. In order to equally share the current, a dynamic consensus algorithm (DCA) based current sharing scheme is proposed in this paper.

Based on the analysis and grid code requirements, a control scheme is proposed to make the MGs not only to maintain connected with the utility grid under voltage sags, but also to support the grid voltage by reactive current injection with accurate power sharing among the distributed converters. This paper is organized as follows. Section II presents the analysis of voltage and current phasors while Section III illustrates the overall hierarchical control scheme. Experimental results is analyzed and discussed in Section IV. Finally, the conclusion of the paper is presented in Section V.

This work is supported by Energy Technology Development and Demonstration Program (EUDP) through the Sino-Danish project "Microgrid Technology Research and demonstration (meter.et.aau.dk)" and Chinese foundation "2014DFG62610".

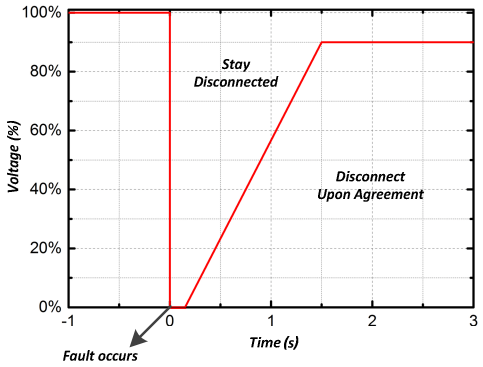

Fig. 1. Requirements of LVRT ability

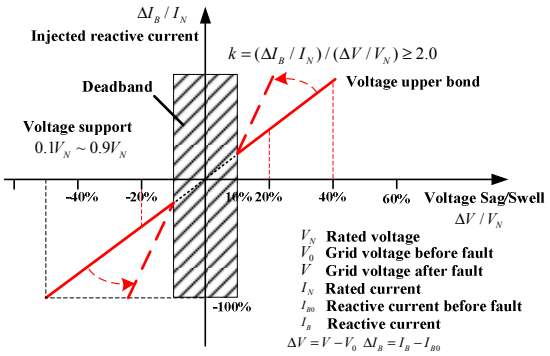

Fig. 2. Reactive power support

II. Power Flow Analysis

The power flow between the converter and the grid is shown in Fig. 3, where v_g and v_{DG} are the grid voltage and converter voltage, respectively. Z_g and Z_o are the grid and the converter closed loop output impedance, respectively. I_g, I_L and I_{INV} are the grid, load and inverter current, respectively.

In this paper, a stiff, mainly inductive grid is considered, and then the classic droop control theory can be obtained where the active power P predominately depends on the power angle δ and the reactive power Q predominately relies on the voltage difference, as shown in (1) and (2). Consequently, by tuning the phase angle and the voltage amplitude, the injected active and reactive powers can be controlled [9].

$$P \approx \frac{EV}{Z}\sin\delta \tag{1}$$

$$Q \approx \frac{EV}{Z}\cos\delta - V^2 \tag{2}$$

The phasor diagram of the grid-interactive system is illustrated in Fig. 4. It can be seen from Fig. 4(a) that before the voltage sag occurs the converter not only supplies active and reactive power to the loads, but also feed some active power to the grid. When the voltage sag appears, the converter will participate on the reactive power support by tuning its output voltage based on (2) and the corresponding phasor diagram is depicted in Fig. 4(b), where v_{sag} is the voltage sag; $I_{injected}$ and v_{com} are the compensated current and voltage, respectively; v_{Lg}

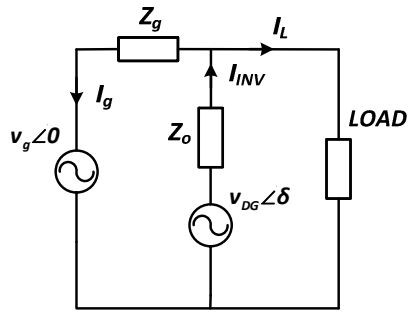

Fig. 3. Equivalent power circuit for DG converter connected to the grid

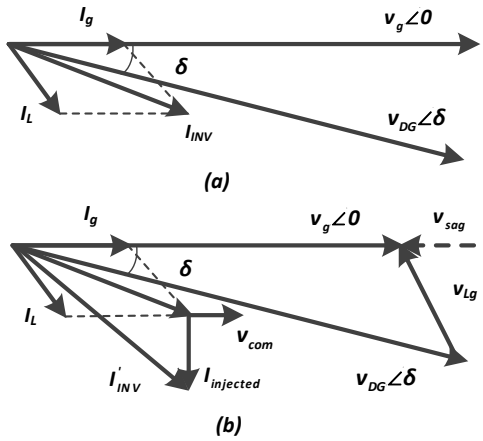

Fig. 4. Phasor diagram of the grid-interactive converter (a) without voltage sag (b) with a voltage sag of 0.2 p.u.

is the grid impedance voltage drop while I_{INV} is the converter output current. Also, the grid current can be calculated as:

$$I_g = \frac{v_{DG}\angle\delta - v_g\angle 0}{Z_g} \tag{3}$$

It can be seen from (3) that the grid current is inversely proportional to the grid impedance Z_g. Thus, an extra inductor can be implemented between the MG and the grid to limit the grid current.

III. Grid-Interactive MG Operation under Grid Faults

A hierarchical control algorithm which consists of primary and secondary level is proposed to achieve LVRT and reactive power sharing in this paper. The overall control schematic diagram is shown in Fig. 5.

A. Primary Controller

Primary controller includes voltage/current inner loop, droop control loop and virtual impedance loop. The voltage/ current inner loop will ensure a good voltage and current waveform, while the droop control loop is used to achieve power sharing. Besides, the converter output current and capacitor voltage is sensed to calculate the active and reactive power based on instantaneous power theory. The calculated active power P and reactive power Q are then fed to the droop controller for power sharing and circulating current

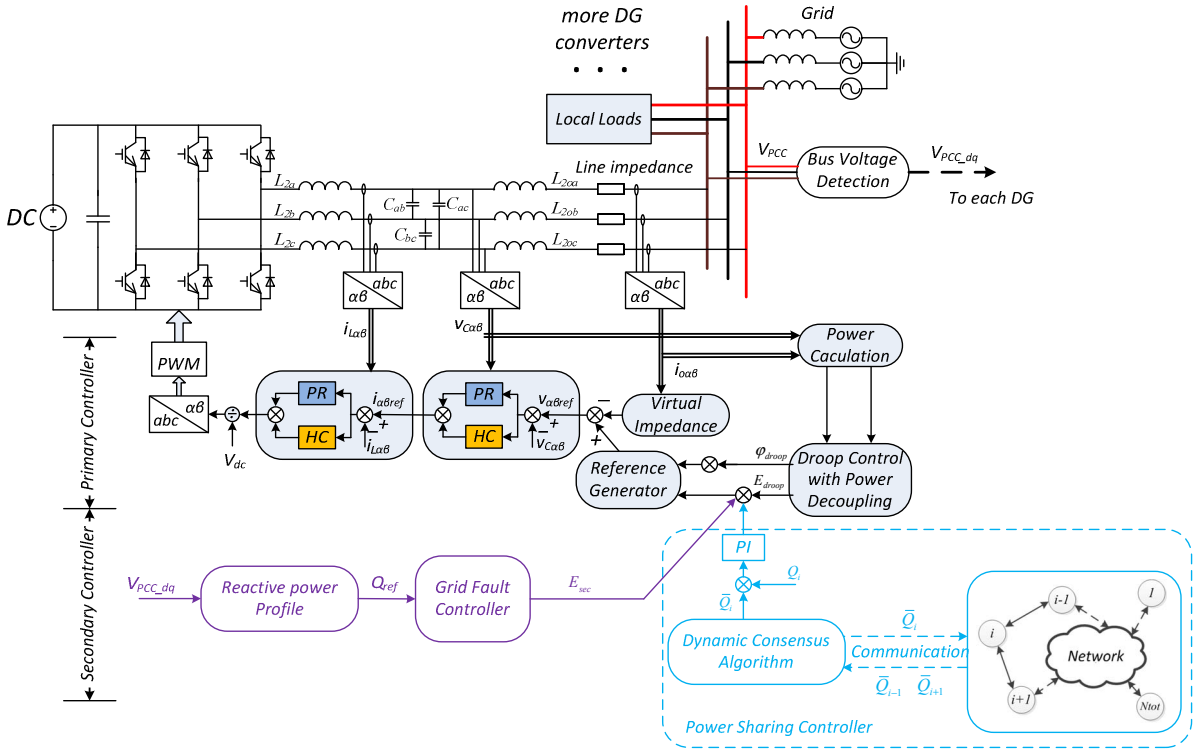

Fig. 5. Hierarchal control scheme

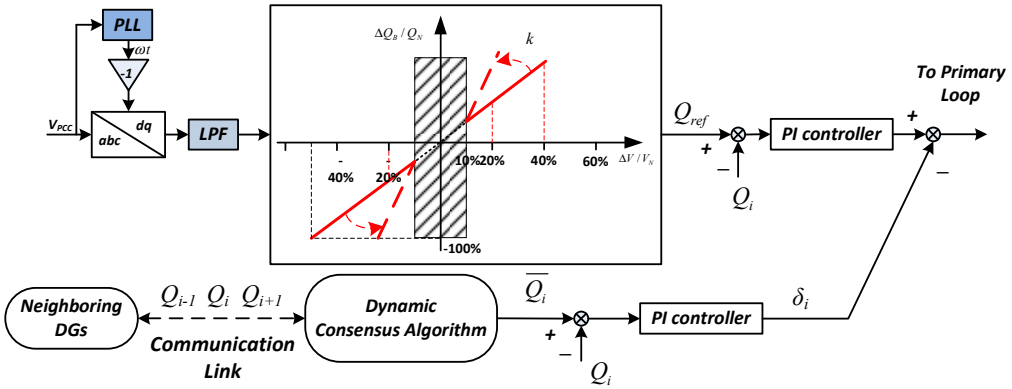

Fig. 6. Secondary control loop

suppression. The droop law in this paper is defined as follows:

$$\varphi^* = \varphi_0 - \left(m_p + \frac{m_I}{s} \right)\left(P - P_{ref} \right) \tag{4}$$

$$E^* = E_0 - n_p \left(Q - Q_{ref} \right) \tag{5}$$

where φ^* and E^* are the amplitude and phase angle of the voltage reference while E_0 and φ_0 are the nominal value of the voltage amplitude and phase angle, P_{ref} and Q_{ref} are respectively the reference of active and reactive power, m_p, m_I and n_I are the proportional and integral coefficients for the power controllers, respectively.

In addition, the virtual impedance loop is implemented since it makes the system more damped and provides better *P/Q* decoupling with appropriate output impedance shaping [9]. Note that all the primary loop controllers are implemented in $\alpha\beta$ reference frame along with proportional-resonant (*PR*) controller [10].

B. Secondary Controller

Secondary controller mainly takes care of the reactive power injection and its sharing between the distributed converters. As shown in Fig. 6, the three phase load voltage is first measured to obtain the voltage amplitude in *dq* reference frame. Then, the reactive power reference Q_{ref} is generated according to the red curve in Fig. 6 and is afterwards send to a *PI* controller to calculate the voltage reference signal E_{sec}. Finally, the calculated reference E_{sec} is sent to the local primary controller through communication links. It is worth noting that since high bandwidth low pass filter (*LPF*) is implemented

$$L=\begin{bmatrix}1 & -1\\ -1 & 1\end{bmatrix}$$

Fig. 7. Adopted communication topology and the corresponding Laplacian matrix

here, a faster dynamic response can be obtained compared with conventional droop control.

In order to decouple the reactive power sharing accuracy with the line admittance, the power sharing controller compares the reactive power (Q_i) of each DG with averaged reactive power ($\bar{Q}_i$) value from all DG sides. Q_i is calculated by local controllers, while $\bar{Q}_i$ is obtained by using DCA.

The control scheme and the power references are shown as follows:

$$E_{\text{sec}} = PI(s)\times\left(Q_{ref}-Q\right) \tag{6}$$

$$Q_{ref}=\begin{cases}0, & V_g > 0.9V_N\\ \left(-k\times\dfrac{V_g}{V_N}+k\right)\times Q_N, & 0.9V_N > V > 0.5V_N, k\geq 2\\ Q_N, & V_g \leq 0.5V_N\end{cases} \tag{7}$$

where E_{sec} is the control signal sent to converter primary controller, Q is the reactive power injected by the converter while Q_N is the converters power capacity, Q_{ref} is the reactive power reference which is defined in accordance to the grid code.

C. Dynamic Consensus Algorithm

In cooperative control of multiple distributed agents, in order to reach their common goals, these agents need to reach an agreement on certain quantities of interest by exchanging information through communication links [11]. Note that only communication links between neighboring agents are required.

The general form of the consensus algorithm can be presented as [12]:

$$x_i(k+1)=x_i(k)+\sum_{n\in N_i}a_{ij}(x_j(k)-x_i(k)) \tag{8}$$

where i are the indexes of agent nodes. $x_i(k)$ and $x_i(k+1)$ are the information obtained from agent i at k^{th} and $(k+1)^{\text{th}}$ iteration, respectively. a_{ij} is the edge weight between node i and node j. N_i is the set of indexes of the agents that are connected with agent i.

According to [12], the matrix form of (8) can be expressed as:

$$X(k+1)=W\cdot X(k) \tag{9}$$

where $\boldsymbol{X}(k)=[x_1(k), x_2(k), \ldots, x_{NoC}(k)]^T$, $\boldsymbol{W}$ is the weight matrix of the communication network and N_{oC} is the total number of agent nodes.

In this paper, a modified version [13-14] of the above mentioned algorithm, namely dynamic consensus algorithm, is applied to obtain a convergence in environment with dynamically changing variables. This algorithm can be expressed as:

$$x_i(k+1)=x_i(0)+\varepsilon\cdot\sum_{j\in N_i}\delta_{ij}(k+1) \tag{10}$$

$$\delta_{ij}(k+1)=\delta_{ij}(k)+a_{ij}\cdot\left(x_j(k)-x_i(k)\right) \tag{11}$$

where ε is the constant edge weight between agents. $\delta_{ij}(k)$ stores the cumulative difference between two agents, and $\delta_{ij}(0)=0$. Note that $a_{ij}>0$, only when agent i and agent j are neighbors.

In this paper, $x(k)$ stands for the discovered average value of reactive power, and $x(0)$ means the local measured reactive power. Accordingly, DCA helps each local unit to discover the global average of reactive power.

Also, constant edge weight is adopted and is defined as:

$$W=I-\varepsilon\cdot L \tag{12}$$

where L is the Laplacian matrix of the communication topology.

Since bidirectional and symmetrical iteration is considered in the paper, then ε can be chosen as follows to obtain fastest possible convergence of the communication algorithm.

$$\varepsilon=\frac{2}{\lambda_1(\mathbf{L})+\lambda_{n-1}(\mathbf{L})} \tag{13}$$

where λ_j denotes the j^{th} largest eigenvalue of a symmetric matrix. Based on the topology of Fig. 5, the eigenvalues of L are $[0\ 2]^T$ which gives the optimal $\varepsilon=1$.

IV. Experimental Results

In order to validate the correctness of the proposed control strategy, experiments have been carried out on a MG platform existing in the Microgrid Lab at Aalborg University [15]. The platform consists of a *dSPACE* 1006 control board and three 2.2kW *Danfoss* three-phase DG converters which share a common AC bus. The detailed electrical configuration is shown in Fig. 5. One converter is programmed to emulate grid while the other two converters act as DG converters. In addition, power stage and control system specifications can be found in Table I. Note that a 5mH inductor is used to emulate the grid impedance as explained in Section II.

The correctness of the proposed control strategy has been tested in the presence of three phase voltage sag of 0.1 p.u. which occurs at t = 0.1s and clears at t = 0.6s (as shown in Fig. 8). In this case, the converter should provide reactive power needed to compensate the voltage sag. During the sag, all the DG converters are controlled to support the voltage, such that the load side voltage can be restored with the greatest extent. It is worth noting that due to the converter capacity limitations,

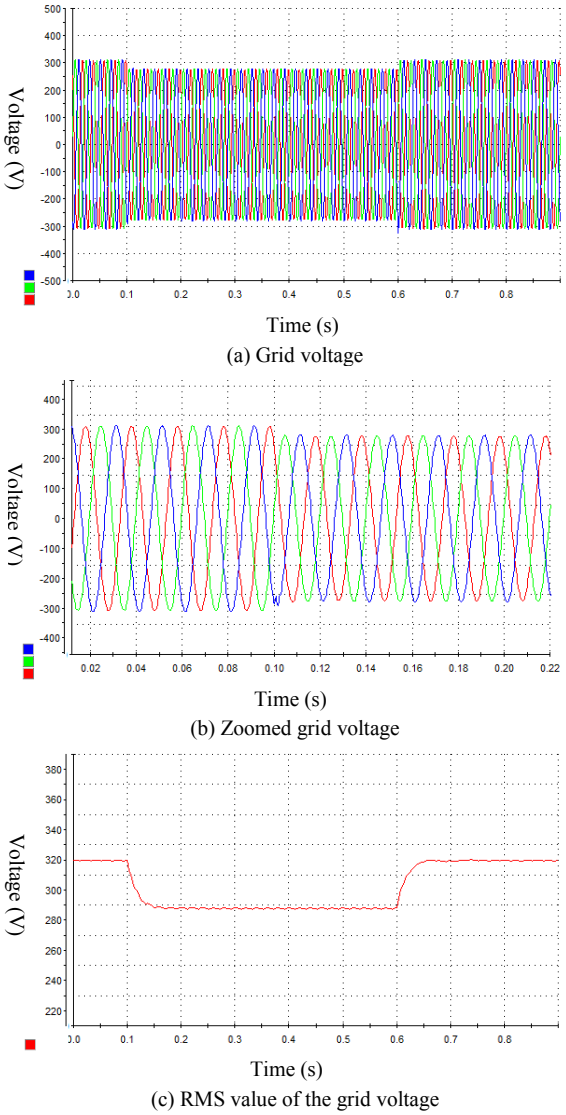

Fig. 8. Grid voltage during a 0.1 p.u. and 500ms voltage sag

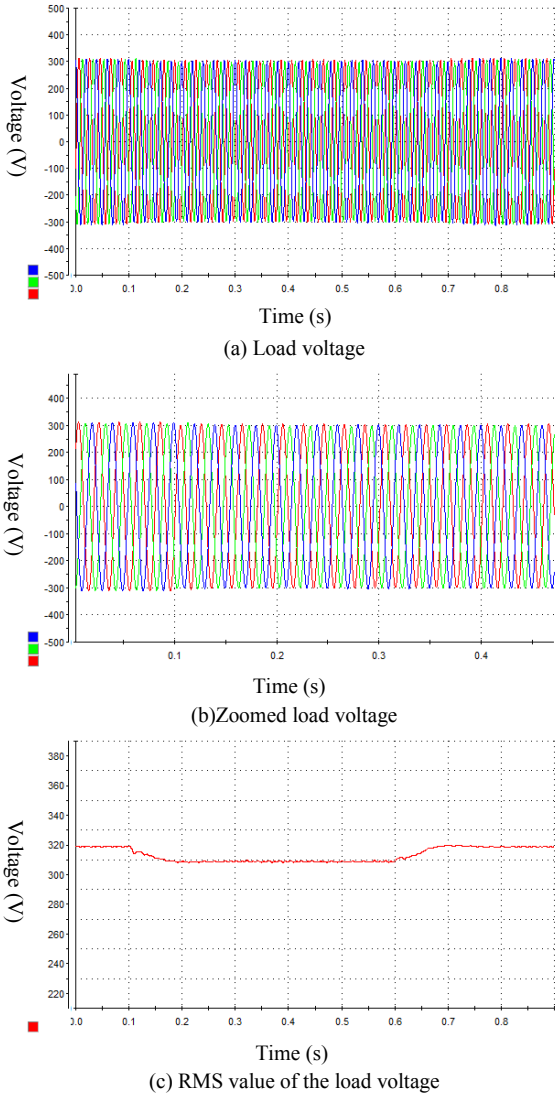

Fig. 9. Load voltage during the voltage sag

the voltage magnitudes is controlled not to achieve exactly the nominal value. Bigger inductors and more available DG capacity will help restoring the grid voltage, as explained before.

Fig. 9 depicts three phase load voltage during the voltage sag. Obviously, the grid voltage decreases from 320V to 290V while load voltage only decrease from 320V to 310V.

The reactive powers injected to the grid by the two converters are shown in Fig. 10. Note that the k value in (4) is set to 7 which means that 1% drop of the grid voltage requires at 7% increase of the rated current, i.e. Q_{ref} is 1540Var.

Fig. 11 shows the grid current waveform. It can be seen that the current regulation time is only four to five cycles which is fast enough to ride through the grid faults.

As it can be seen from Fig. 10 and 11, the converter can provide appropriate amount of power according to the depth of the voltage sag within five cycles. In such a way, the grid

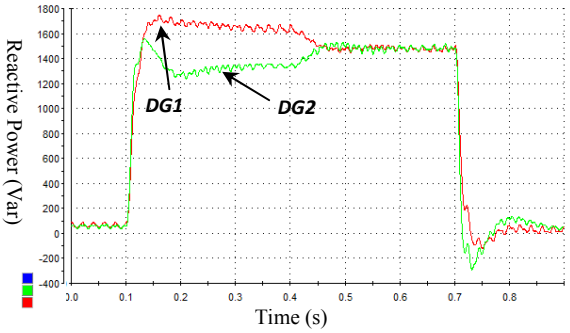

Fig. 10. Reactive power injected by the two DG converters

voltage can be restored and the customer side electrical equipment can be protected from potential damage.

In order to eliminate the effect of line admittance to power sharing accuracy, the DCA based power sharing controller is activated at t =0.4s. It can be seen from Fig. 11 that after t = 0.4s, the reactive power converge to the average value within

TABLE I. POWER STAGE AND CONTROL SYSTEM PARAMETERS

Parameters of the Power Stage			
Parameters	**Symbol**	**Value**	**Unit**
Grid Inductance	L_g	*1.8*	*mH*
LCL filter Inductance	L_f	*1.8*	*mH*
Filter Capacitance	C	*9*	*μF*
Nominal Voltage	V	*230*	*V*
Nominal Frequency	f	*50*	*Hz*
DC Voltage	V_{DC}	*650*	*V*
Switching Frequency	f_s	*10*	*kHz*
Line admittance of DG1	Y_{L1}	*0.7-j0.42*	*S*
Line admittance of DG2	Y_{L2}	*0.36-j0.25*	*S*
Voltage/Current Inner Loop Controllers			
Parameters	***Symbol***	***Value***	
Voltage Loop Controller	k_{vp}, k_{vr}	*0.05, 30*	
Current Loop Controller	k_{ip}, k_{ir}	*2, 200*	
Primary Controller			
Parameters	***Symbol***	***Value***	***Unit***
Proportional Phase Droop	m_P	*0.0005*	*Rad·s/W*
Integral Phase Droop	m_I	*0.00006*	*Rad/W*
Proportional Phase Droop	n_P	*0.002*	*V/Var*
Virtual Resistor	R_v	*1*	*Ω*
Virtual Inductor	L_v	*4*	*mH*
Secondary Controller			
Parameters	***Symbol***	***Value***	
Proportional Components	k_p	*0.01*	
Integral Components	k_I	*0.02*	
constant edge weight	ε	*1*	

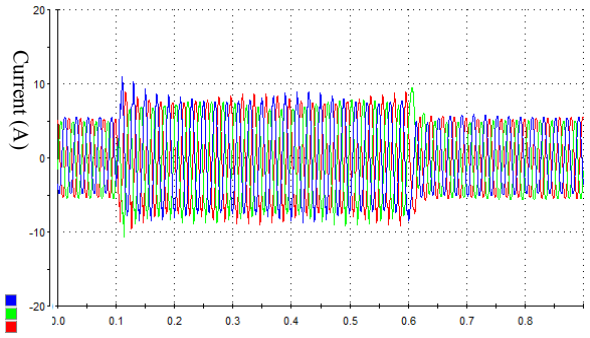

(a) Grid current

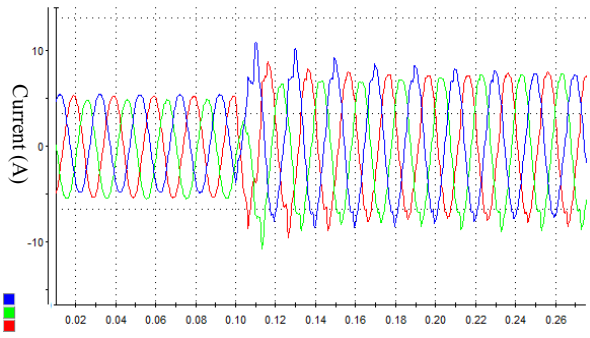

(b) Zoomed grid current

Fig. 11. Grid current during the voltage sag

0.1s. This means the DCA helps each agent to converge to the same average value. Note that sample time of the communication link is 0.0001s, since LVRT usually needs a fast response.

V. CONCLUSIONS

In this paper, a distributed low voltage ride through control strategy based on dynamic consensus algorithm for grid-connected MGs has been investigated. The power flow of the system is investigated to develop the voltage sag compensator, and then the reactive power sharing controller is introduced to decouple the injected power and the line admittance. Experimental test bed which contains two DG converters and the grid are constructed to validate the proposed control strategy. The experimental results show that the proposed control strategy endows the MG system with low voltage ride-through capability as well high power sharing accuracy.

REFERENCES

[1] P. Basak, A. K. Saha, S. Chowdhury, S. P. Chowdhury, "Microgrid: Control techniques and modeling," IEEE Universities Power Engineering Conf., pp. 1-5, Sep. 2009.

[2] N. Jelani, M. Molinas, S. Bolognani, "Reactive Power Ancillary Service by Constant Power Loads in Distributed AC Systems," IEEE Trans. Power Del., vol. 28, no. 2, pp. 920-927, Feb. 2013.

[3] E. ON GmbH, "Grid Code - High and extra high voltage." [Online]. Available: http://www.eon-netz.com/.

[4] E. Saiz-Marin, J. Garcia-Gonzalez, J. Barquin, E. Lobato, "Economic Assessment of the Participation of Wind Generation in the Secondary Regulation Market," IEEE Trans. Power Syst., vol. 27, no. 2, pp. 866-874, Jan. 2012.

[5] X. Guo, W. Liu, X. Zhang, X. Sun; Z. Lu; J. M. Guerrero, "Flexible Control Strategy for Grid-Connected Inverter Under Unbalanced Grid Faults Without PLL," IEEE Trans. Power Electron., vol. 30, no. 4, pp.1773-1778, April 2015.

[6] Y. Yang, F. Blaabjerg, Z. Zou, "Benchmarking of Grid Fault Modes in Single-Phase Grid-Connected Photovoltaic Systems," IEEE Trans. Ind. Appl., vol. 49, no. 5, pp. 2167-2176, Sept.-Oct. 2013.

[7] X. Bao, P. Tan, F. Zhuo, X. Yue, "Low voltage ride through control strategy for high-power grid-connected photovoltaic inverter," IEEE Applied Power Electronics Conference and Exposition (APEC), pp. 97-100, March 2013.

[8] S. Hu, X. Lin, Y. Kang, X. Zou, "An Improved Low-Voltage Ride-Through Control Strategy of Doubly Fed Induction Generator During Grid Faults," IEEE Trans. Power Electron., vol. 26, no.12, pp. 3653-3665, Dec. 2011.

[9] J. C. Vasquez, R. A. Mastromauro, J. M. Guerrero, M. Liserre, "Voltage Support Provided by a Droop-Controlled Multifunctional Inverter," IEEE Trans Industrial Electron., vol. 56, no. 11, pp. 4510-4519, Nov. 2009.

[10] D. N. Zmood, D. G. Holmes, "Stationary frame current regulation of PWM inverters with zero steady-state error," IEEE Trans. Power Electron., vol. 18, no. 3, pp.814-822, pp. 814-822, May 2003.

[11] F. Xiao, L. Wang, "Asynchronous Consensus in Continuous-Time Multi-Agent Systems With Switching Topology and Time-Varying Delays," IEEE Trans. Automatic Control, vol. 53, no. 8, pp. 1804-1816, Sept. 2008.

[12] R. Olfati-Saber, J. A. Fax, R. M. Murray, "Consensus and Cooperation in Networked Multi-Agent Systems," in Proc. IEEE, vol. 95, no. 1, pp. 215-233, Jan. 2007.

[13] L. Meng, X. Zhao, F. Tang, M. Savaghebi, T. Dragicevic, J. Vasquez, J. Guerrero, "Distributed Voltage Unbalance Compensation in Islanded Microgrids by Using Dynamic-Consensus-Algorithm," IEEE Trans. Power Electron., vol. PP, no.99, pp. 1-1.

[14] M. Kriegleder, "A Correction to Algorithm A2 in 'Asynchronous Distributed Averaging on Communication Networks'," IEEE Trans. Networking, vol. 22, no. 6. pp. 2026-2027, Dec. 2014.

[15] Microgrid Research Programme. URL: www.microgrids.et.aau.dk.